



Selective oxidation of alkylarenes to aromatic acids/ketone in water by using reusable binaphthyl stabilized Pt nanoparticles (Pt-BNP) as catalyst

Rajib Saha¹, Govindasamy Sekar*

Department of Chemistry, Indian Institute of Technology Madras, Chennai 600036, India



ARTICLE INFO

Keywords:
 Platinum nanoparticles
 Toluene oxidation
 Heterogeneous catalysts
 Benzoic acid
 Reusable catalyst
 Aromatic ketone
 Aromatic acid
 Water as solvent

ABSTRACT

An efficient methodology for the selective and controlled oxidation of petroleum waste methylarenes/alkylarenes to aromatic carboxylic acids/ketone using easily recoverable and recyclable binaphthyl stabilized Pt nanoparticles (Pt-BNP) as a catalyst has been developed. The greener oxidant *aq. tert*-butyl hydroperoxide (TBHP) and green solvent water have been utilized in this oxidation reaction. The methodology is well tolerated with different functional groups. The less reactive electron deficient toluenes are also oxidized by Pt-BNP and gave a good yield of corresponding carboxylic acids with a high turnover number (TON) 738–1448. The Pt-BNP catalyst was recovered and reused up to five catalytic cycles. The heterogeneous test suggested that the reaction is catalyzed by heterogeneous Pt-BNP catalysts. Based on control experiments and literature reports, a possible reaction mechanism has been proposed.

1. Introduction

Selective oxidation of aromatic hydrocarbons is highly important in both academia and industry [1–6]. From economic as well as environmental point of view, oxidation of hazardous petroleum by-product such as toluene and volatile organic compounds (VOCs) to other useful chemicals is gaining more interest [7–12]. The unselective oxidation of toluene gives a mixture of oxidized products including benzyl alcohol, benzaldehyde, benzoic acid, benzoate ester and phenol [13–15]. Benzoic acid, and its sodium and potassium salts are used as food preservative materials. Also, it has high demand in chemical, pharmaceutical, and agricultural industries as carboxylic acid moiety can be easily converted into other functional groups such as amide, ester, acid chloride, alcohol, iodide etc. by a simple chemical operation [16–20].

Due to the high demand of benzoic acid, the attention is being drawn towards the synthesis of benzoic acid from different types of readily available chemicals such as benzyl alcohol, benzaldehyde, benzoic acid chloride, benzamide, benzoate esters, benzonitrile, toluene, etc. [21–27]. Among all, the synthesis of benzoic acid from naturally abundant toluene is in high demand till date [28–30]. In industry, toluene is oxidized to benzoic acid in the presence of homogeneous catalysts at high temperature and pressure. The most common method is “Dow toluene air oxidation process.” In this process, soluble

cobalt naphthenate catalyst is used for oxidation of toluene in air under 40–70 psi pressure at 150 °C [31]. Another popular method in the industry for the synthesis of commercial benzoic acid is the use of homogeneous cobalt acetate catalyst at high temperature and pressure of molecular oxygen and bromide as a promoter with acetic acid as solvent [32–34]. Use of acetic acid as solvent and bromide as promoter creates difficulty in separation of product and catalyst. Also, a large volume of toxic waste is produced, making this process environmentally and economically unfavourable.

Therefore, many attempts were made to oxidize toluene in vapour phase condition in presence of a solid catalyst to make an environmentally benign process (See SI, Table S1) [35–38]. The use of liquid phase oxidation process has advantages such as easy operation and achieving high selectivity under mild reaction conditions. Many efforts have been made to improve the efficiency of oxidization of toluene in the liquid phase using a homogeneous catalytic system in a volatile organic solvent [38–41]. However, greater selectivity is observed when the conversion is low; when the conversion is high, over-oxidation to CO₂ and other by-products have been observed [42–45]. Thus, there is a need to develop a selective oxidation reaction that avoids over-oxidation and side-products formation, where naturally abundant greener solvent such as water can be used as a solvent under mild reaction condition making it an environmentally benign process.

Recently, the use of the heterogeneous catalyst has shown several

* Corresponding author.

E-mail address: gsekar@iitm.ac.in (G. Sekar).

¹ Dedicated to Padma Shri Prof. Vinod K. Singh on the occasion of his 60th birthday

advantages over a homogeneous catalyst, as it can be easily recovered from the reaction mixture and reused for several catalytic cycles [46–49]. Recently, several attempts have been employed for the oxidation of toluene with environment-friendly oxidants such as TBHP, H_2O_2 or molecular oxygen with heterogeneous transition metal or metal oxide catalyst in replacement of their homogeneous counterparts [50–55] (Also see SI, Table S1). However, most of the catalysts showed poor turn over number (TON) even at a higher temperature [56–58]. Hence, there is a need to develop a catalyst with high TON at low temperature with high selectivity of acid production (See SI, Table S1). From the TON point of view of a heterogeneous catalyst, metal nanoparticles have gained importance due to their high catalytic activity with low particle size and high surface area [59–65]. In 2011, Hutching et al. have reported [66] the oxidation of toluene with molecular oxygen as an oxidant using AuPd supported catalyst at 120–160 °C.

In literature, there are only very few reports available for the selective oxidation of toluene to benzoic acid using TBHP as oxidant at lower temperatures. Compared to other metal oxidants, TBHP is economic and avoids the formation of waste. Lingaiah et al. have reported vanadium substituted polyoxometalate catalysts for oxidation of toluene to benzaldehyde using TBHP as oxidant [67]. Hutchings et al. have used 1% Au-Pd/TiO₂ for toluene oxidation to yield a mixture of products at 80 °C [68]. Alternatively, the platinum group metal catalysts are well known for the oxidation of hydrocarbons [69–75]. Recently, Shimizu and co-workers have reported a supported platinum catalyst for solvent free synthesis of ester from primary alcohols under N_2 at 180 °C [76].

Our continuous efforts towards the metal nanoparticles catalyzed organic transformations, [77–81] here in we report binaphthyl backbone stabilized Pt-nanoparticles (Pt-BNP) as a catalyst for the selective oxidation of petroleum waste toluene to benzoic acid with high conversion and TON.

2. Experimental section

2.1. Catalyst preparation

The platinum nanoparticles were synthesized by two steps procedure. First, [1,1'-binaphthalene]-2,2'-diamine (BINAM) was diazotised using HBF_4 and $NaNO_2$. Then, the diazonium salt was treated with H_2PtCl_6 in acetonitrile, followed by reduction of Pt(IV) by $NaBH_4$ which resulted in Pt nanoparticles (Scheme 1). Simultaneously, the heat generated from the reduction leads to the generation of binaphthyl radical which stabilizes the nanoparticles via strong Pt-C linkage. Different type of Pt-NPs with different stabilizers such as phenyl (Pt-PNP), 1-naphthyl (Pt-NNP) and 8-quinonyl (Pt-QNP) have been synthesized using the above mention procedure. The details experiment procedure for the synthesis of Pt-NPs is given in SI.

2.2. Characterization of catalyst

The formation of platinum nanoparticles was confirmed by UV spectroscopy using SHIMADZU UV-3100 spectrophotometer and quartz cuvette with a 10 mm path length. Size and shape of the Pt-NP was analyzed with (HR-TEM) JEOL-3010 transmission electron microscope operating at 300 kV. which showed the particle size in the range between 4–8 nm. Samples for HR-TEM were prepared by dispersing the

powdered sample in dichloromethane (DCM) by sonication and then drip drying on a copper grid (200 mesh) coated with carbon film. To determine the binaphthyl moieties present in the nanoparticles as stabilizer, FTIR analysis using Jasco FT/IR-4100 and solid state NMR data were obtained using high resolution 400 NMR (Bruker). The crystalline structure of the platinum nanoparticles was determined by X-ray diffraction analysis using D8 advance (Bruker) X-ray diffractometer instrument at room temperature. The latter appeared with $Cu K\alpha$ (1.5406 Å) voltage: 40 kV, current: 30 mA and was in the range of 10–80 (20). All the peaks in PXRD pattern were assigned and compared with the database published by JCPDS. The X-ray photoelectron spectroscopy (XPS) was conducted on an XPS analysis (Omicron ESCA Probe spectrometer) equipped with monochromatic $Mg K\alpha$ (1253.6 eV). The binding energy was calibrated using the C 1s photoelectron peak at 284.8 eV as a reference (see SI). The elemental composition in the reaction mixture was determined by EDX analysis. The quantity of Pt content (1.6 wt%) in nanoparticle was determined by ICP-OES analysis using Perkin Elmer Optima 5300 DV.

2.3. Catalytic reaction

Under open atmosphere, toluene **1** (0.5 mmol), 0.066 mol% (8 mg) of Pt-BNP (1.6 wt% Pt by ICP-OES analysis), 70% aqueous TBHP (2.0 mmol) and nanopure water (1.0 mL) were successively added to oven dried reaction tube then the reaction tube was fitted with oxygen balloon. Nano pure water was obtained from Barnstead nanopure water system. Then the reaction tube was immersed in an 80 °C pre-heated oil bath and stirred with a stir bar till complete consumption of toluene. Upon cooling down to room temperature, the reaction tube was washed with ethanol, and the liquid was added to the collection vial. The internal standard substance naphthalene was also added to the collection vial. The samples were analyzed by GC (Shimadzu GC-2010) equipped with FID and Stabilwax®-DA, capillary column (35 m, 0.32 mmID, 0.25 um).

The conversion (%) of toluene was calculated using the standard procedure:

Conversion % of toluene

$$= \frac{(Initial \text{ moles of toluene} - \text{moles of toluene remained after the reaction})}{(initial \text{ moles of toluene for the reaction})} \times 100$$

The yield (%) of acid was calculated using this formula:

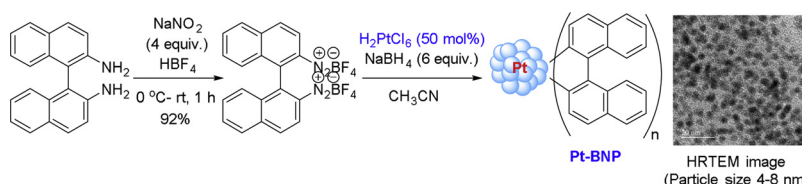
$$\% \text{yield of acid} = \frac{\text{moles of acid formed}}{\text{initial moles of toluene for the reaction}} \times 100.$$

The TON (turn over number) of catalyst was calculated using the formula:

$$TON = \frac{\text{mole of product formed}}{\text{mole of catalyst used for the reaction}}$$

2.4. Experimental procedure for reusing of Pt-BNP catalyst

To reuse the Pt-BNP catalyst, the reaction was repeated with 4-methoxy toluene **1a** as a substrate in 1.0 mmol scale retaining identical conditions, except the usage of Pt-BNP catalyst rather than fresh catalyst. After the completion of 4-methoxy toluene oxidation reaction, the



Scheme 1. Synthesis of Pt nanoparticles (Pt-BNP).

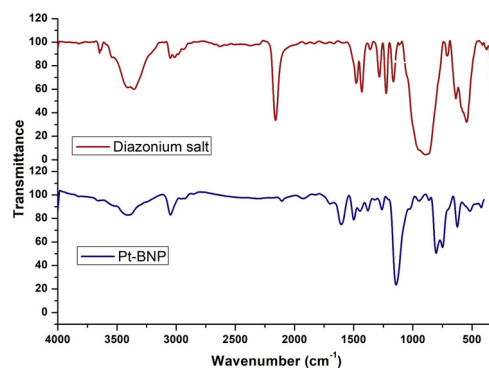


Fig. 1. IR spectrum of both BINAM diazonium salt and Pt-BNP.

reaction mixture was allowed to cool to room temperature. EtOH (2 mL) was added to the reaction mixture and centrifuged. The liquid was decanted to a 50 mL conical flask. Again EtOH (5 mL) was added and centrifuged and decanted to the same conical flask. This procedure was repeated up to three times. After that, the catalyst was washed with nano pure water (5 mL) and ethanol (5 mL) two times. Finally, the resulting solid residue (Pt-BNP) dried under vacuum. The dried catalyst was reused for further catalytic cycle. The collected liquid was concentrated by reduce pressure. The resulting reaction mixture was purified by column chromatography on silica gel (hexanes: ethyl acetate) to afford **4a** as the desired product.

3. Results and discussion

3.1. Characterization of Pt-BNP

Inferences were drawn from the comparison of FTIR spectra of the Pt-binaphthyl NPs (Pt-BNP) with the corresponding BINAM diazonium salt. The absence of absorption band at 2263 cm^{-1} in the Pt NPs indicated the absence of the diazonium group in the synthesized NPs (Fig. 1). The bands at 3048 cm^{-1} and 2925 cm^{-1} in Pt-BNPs corresponds to the stretching vibrations of aromatic C–H. The bands at 805 , 751 and 621 cm^{-1} are ascribed to C–H bending and peaks at 1600 and 1505 cm^{-1} are because of C=C vibrations. All these data confirmed the presence of the binaphthyl moiety in the synthesize Pt-BNPs.

In UV-vis spectra, we found a peak at 278 nm correspond to the platinum nanoparticle. And peaks at 346 nm , 362 nm and 411 nm corresponding to organic aromatic binaphthyl stabilizer of NPs. The peak corresponds to the H_2PtCl_6 and PtCl_4 at 262 nm , 327 nm and 393 nm respectively are completely disspread from the NPs which shows that the platinum metal salt completely converted to NPs (Fig. 2).

Further ^{195}Pt NMR study has been carried out for characterization of Pt-BNP. Two broad peaks were observed at -2769 and -2346 ppm in ^{195}Pt NMR. The oxidation of platinum atom from lower Pt(0) to higher

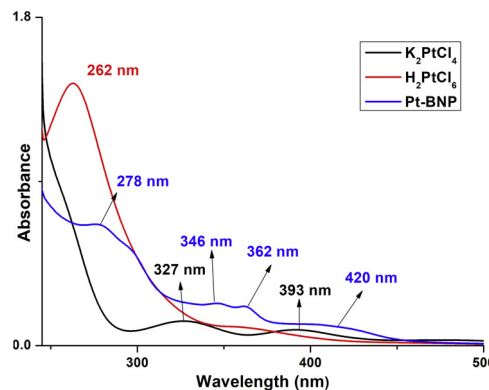


Fig. 2. UV-vis spectrum of Pt-BNP.

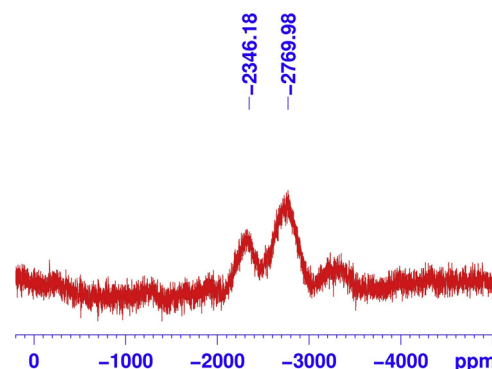


Fig. 3. ^{195}Pt NMR of Pt-BNP in CDCl_3 (107 MHz).

Pt(II) changes by removal of electrons, it leads to deshielding and thus, high-frequency shifts are observed. [82] When the binaphthyl moiety binds on the surface atom of NPs through covalent bond, the binaphthyl binding metal atom attains to the higher oxidation state. That may be the reason for two broad peaks at -2769 and -2346 ppm in ^{195}Pt NMR. The intensity of peak at -2346 ppm is lower compared to the peak at -2769 ppm which indicates that less number of Pt atom may bind with binaphthyl moiety. There are no peaks corresponding to the H_2PtCl_6 and PtCl_4 complex, which showss that the platinum salts are completely converted to the Pt-NPs during the preparation of NPs (Fig. 3).

The crystalline nature of Pt-BNP has proved from powder XRD data. In powder XRD pattern of Pt-BNP, peaks found at 31.9 , 33.9 , 39.8 , 45.1 , 45.9 , 67.4 and 81.6 which corresponds to peak Pt_3O_4 (100), PtO (101), Pt (111), PtO (102), Pt (200), Pt (220) and Pt (311) respectively (JCPDS number are 751060, 850714 and 882343) (Fig. 4). Latter using the Debye-Scherrer equation from P-XRD calculated the particle size of Pt-BNP, the average particle size is 7.0 nm (See SI). The result quite agrees with HRTEM analysis data of particle size.

HRTEM images of Pt NPs revealed that most of the particles are spherical in shape and are well dispersed on the TEM grid without any apparent aggregation. The Pt NPs have a particles size distribution of $4\text{--}8\text{ nm}$ (Fig. 5). High resolution TEM images divulged a well-defined lattice fringe of 0.20 nm which is accredited to the lattice plane (Fig. 6).

The oxidation state of Pt atom in Pt-BNP was confirmed by XPS analysis. The XPS investigation of Pt 4f region ($\text{Pt } 4f_{7/2}$ and $\text{Pt } 4f_{5/2}$) revealed that the binding energy values for $\text{Pt } 4f_{7/2}$ and $\text{Pt } 4f_{5/2}$ lines in Pt nanoparticle core are 71.0 and 74.4 compared with pure platinum metal. The binding energy of $\text{Pt}^{2+} 4f_{7/2}$ and $\text{Pt}^{2+} 4f_{5/2}$ found at 73.9 and 77.2 respectively. From the spectrum (Fig. 7), it was observed that the NPs were present in Pt^0 , Pt^{2+} and Pt^{4+} oxidation state and ratio was found 47 , 36 and 17 respectively. Surface oxidation of Pt to PtO and PtO_2 could be a possible justification to this. In addition, some of the Pt atoms may bond to binaphthyl moieties and resulted in Pt^{2+} oxidation

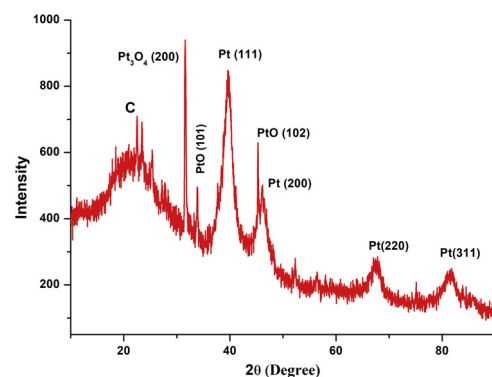


Fig. 4. The powder XRD pattern of Pt-BNP.

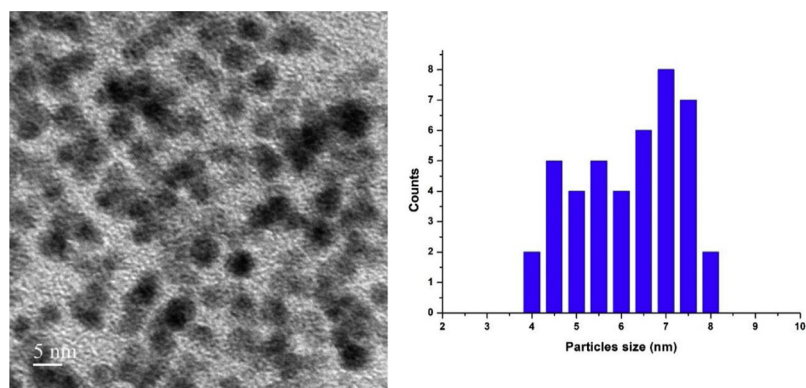


Fig. 5. Depicts the HR-TEM micrographs of Pt BNP and particle size distribution.

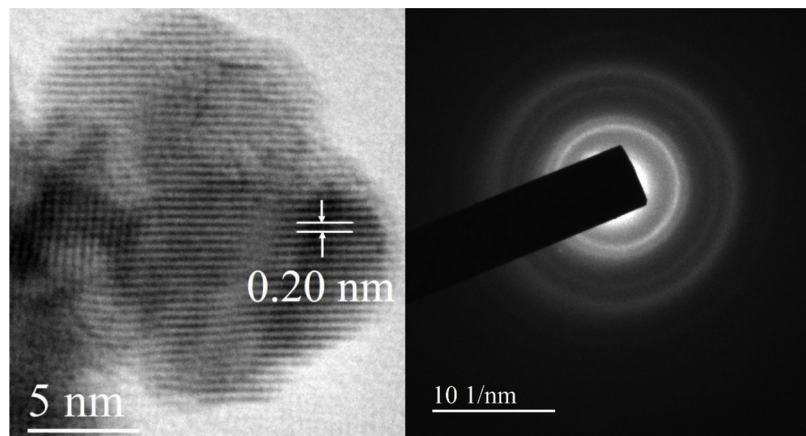


Fig. 6. High-resolution TEM image with defined lattice fringe.

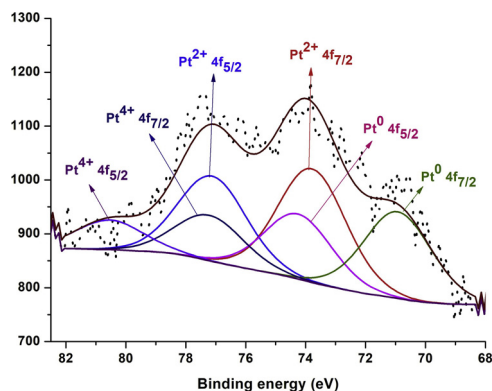


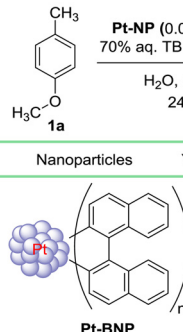
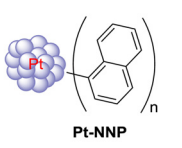
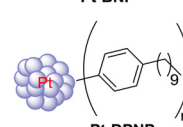
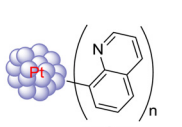
Fig. 7. XPS spectrum of Pt-BNP.

state.

3.2. Oxidation of toluenes

After detailed characterization of synthesized Pt-BNP, it was used as catalyst for oxidation of toluene. The initial investigation was carried out by using 4-methoxy toluene (**1a**) as a model substrate in presence of Pt-BNP (8 mg) catalyst and molecular oxygen as oxidant at 60 °C under solvent-free condition. It was observed that the reaction did not proceed; starting material remained as it is. But, when the reaction was carried out using TBHP as oxidant in water as solvent, it gave 61% yield of corresponding *p*-anisic acid selectively as sole product (Table 1, entry 1). Stimulated by this initial result, the catalytic activity of other stabilized Pt-NP for this toluene oxidation was investigated. Other

Table 1
Pt NPs catalyzed oxidation of toluene.

Nanoparticles	Yield (%) 2a/3a/4a	Nanoparticles	Yield (%) 2a/3a/4a
	1/0/61		1/1/53
	1/2/48		2/0/57

nano particles stabilizers such as phenyl (Pt-PNP), 1-naphthyl (Pt-NNP), and 8-quinonyl (Pt-QNP) have been used to improve the yield of the process. However, these NPs showed only low to moderate activities compared with Pt-BNP. Notably, the homogeneous platinum salts PtCl_2 and K_2PtCl_4 were investigated for the oxidation reaction and they were unable to oxidize the 4-methyl anisole. Further optimization of reaction parameters was studied using Pt-BNP as catalyst and TBHP as an oxidant.

Then, the effect of Pt-BNP catalyst loading for oxidation of 4-methyl anisole to 4-anisic acid was investigated and the results are summarized

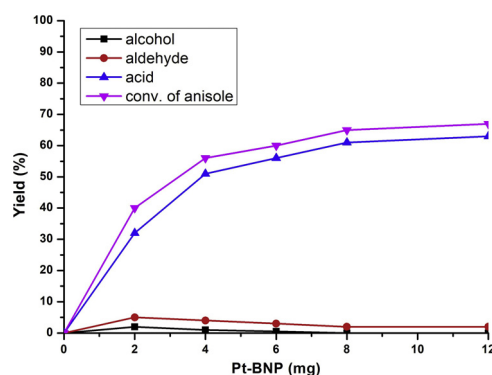


Fig. 8. Pt-BNP catalyst loading effect in toluene oxidation.

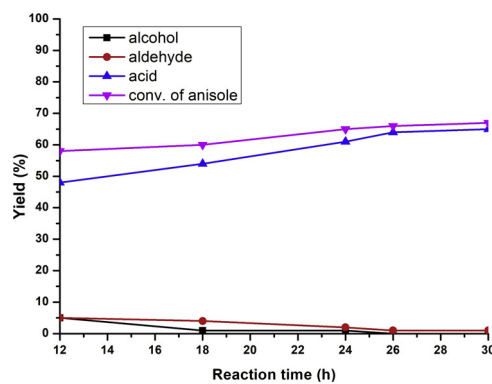


Fig. 9. Effect of reaction time on oxidation of 4-methoxy toluene.

in Fig. 8. Decreasing the catalyst loading from 8 mg (0.064) to 2 mg (0.017 mol%), decreased both the conversion (40%) and formation of the corresponding acid (32%) simultaneously. On further increasing the catalyst loading from 8 mg (0.064) to 12 mg (0.1), the yield of the acid did not increase significantly. In the absence of the catalyst, no product formation was observed.

To improve the yield of acid, further optimization was carried out using 8 mg of Pt-BNP catalyst. Subsequently, the reaction time was investigated. After 26 h, yield and conversion did not increase significantly, this may be due to the lack of oxidant present in the reaction

Table 3
Optimization of reaction in oxygen atmosphere^a.

Entry	Oxidant (equiv.)	Temp. (°C)	Yield (%) ^b		
			2a	3a	4a
1	TBHP (4.0)/ O ₂	60	0.0	3.5	70.0
2	TBHP (2.0)/ O ₂	60	0.0	2.9	65.0
3	TBHP (2.0)/ O ₂	70	0.4	0.8	89.0
4	TBHP (2.0)/ O₂	80	0.0	0.0	95.0
5	TBHP (1.0)/ O ₂	80	0.0	8.0	45.0
6	TBHP (0.5)/ O ₂	80	0.0	3.0	43.0

^a Reaction conditions: **1a** (0.5 mmol), 70% aqueous TBHP with 2 mL solvent in 26 h.

^b Yield was calculated by GC.

mixture. Initially, the reaction generated alcohol which is immediately oxidized to corresponding aldehyde, and finally, the aldehyde was oxidized to acid (Fig. 9).

Then different types of oxidants were used to improve the yield. Except for TBHP, other oxidants such as molecular oxygen, K₂S₂O₈, Na₂S₂O₈, oxone and H₂O₂ were unable to improve the yield of the acid (Table 2, entries 1–5). Then, the reaction was carried out in different solvents such as DCE, DMF, DMSO and THF which were failed to give the acid. The above solvent screening showed that the greener solvent water is the best for the oxidation of 4-methoxy toluene.

The TBHP itself good enough oxidant for conversion of toluene to benzoic acid but the requirement of a large quantity of TBHP which is not economically favourable. To reduce the quantity of TBHP, O₂ has been used for the oxidation of toluene. Surprisingly, when the reaction was carried out under oxygen atmosphere along with TBHP, the yield of acid increased to 70% (Table 3 and entry 1). In the presence of metal, molecular oxygen itself is a good oxidizing agent for oxidation of aldehyde to acid. So the reaction was carried out in the presence of 2 equivalents of TBHP in oxygen atmosphere. As expected, not much variation in yield was observed (entry 2).

Further, the reaction temperature was increased to improve the yield of acid. When the reaction was carried out at 80 °C, the maximum

Table 2
Optimization of reaction parameters^a.

Entry	Catalyst	Oxidant	Solvent	Yield (%) ^b		
				2a	3a	4a
1	Pt-BNP	O ₂	H ₂ O	0.0	0.0	0.0
2	Pt-BNP	K ₂ S ₂ O ₈	H ₂ O	0.0	0.0	0.0
3	Pt-BNP	Na ₂ S ₂ O ₈	H ₂ O	0.0	0.0	0.0
4	Pt-BNP	Oxone	H ₂ O	0.0	0.0	0.0
5	Pt-BNP	H ₂ O ₂	H ₂ O	0.0	0.0	0.0
6 ^c	Pt-BNP	TBHP	–	3.5	3.3	39.0
7	Pt-BNP	TBHP	EtOH	1.1	12.0	18.0
8	Pt-BNP	TBHP	MeOH	2.0	10.0	20.0
9	Pt-BNP	TBHP	THF	0.0	0.0	0.0
10	Pt-BNP	TBHP	DMF	0.0	0.0	0.0
11	Pt-BNP	TBHP	DMSO	0.0	0.0	0.0

^a Reaction conditions: **1a** (0.5 mmol), 70% aqueous TBHP with 2 mL of solvent in 26 h.

^b Yield was calculated by GC.

^c 5.0 M TBHP in decane was used.

Table 4

Substrate scope with electron rich and neutral toluenes ^a .				
Entry	Toluenes	Product	Time (h)	Yield (%)
1			26	95
2			26	86
3			26	79
4			26	75
5			28	81
6			26	92
7			26	95

^a Reaction was carried out in 1.0 mmol scale.

yield was observed as 95% (entry 4). Further reducing the TBHP equivalent was ineffective to increase the yield of acid (entries 5 and 6). So the optimized reaction condition was found to be Pt-BNP (8 mg), TBHP (2 equiv.) under oxygen atmosphere at 80 °C for 26 h.

With this optimized reaction condition in hand, various substituted toluenes were oxidized to corresponding acids and the results are summarized in Tables 4, 5 and 6. Both electron donating and electron withdrawing group substituted toluenes were oxidized to corresponding acids under the optimized condition. The electron rich toluenes took shorter reaction time compared to electron deficient toluene which indicates that electron donating group containing toluene are more active substrates for the oxidation reaction. Electron donating group such as OMe and Me substituted toluene gave a very good yield of acid products (Table 4 and entries 1–4). Electronically neutral substrate such as 1-methyl naphthalene and toluene underwent the optimized reaction condition and yielded the corresponding product 4f and 4g in 92 and 95%, respectively.

Interestingly, halogens such as chloro, bromo and iodo substituted toluene underwent to this oxidation smoothly without affecting halogen group and gave the corresponding acid product in very good yield (Table 5). This halo acid can be utilized for further organic transformations. In the case of 3-chloro toluene, 87% yield of acid 4h was observed. Both *ortho* and *para*-substituted bromo toluene gave 89% and 90% yields of 4i and 4j respectively. The 4-iodotoluene gave less yield compared to 3-iodotoluene, the reason may be the insoluble nature of solid 4-iodotoluene (entries 4 and 5).

In general, oxidation of electron withdrawing group containing toluene is very difficult and there is a need to apply harsh reaction conditions for smooth conversion. The optimized reaction condition was

Table 5

Substrate scope of halogen substituted toluenes ^a .				
Entry	Toluenes	Product	Time (h)	Yield (%)
1			29	87
2			30	89
3			30	90
4			24	91
5			32	77

^a Reaction was carried out in 1.0 mmol scale.

applied to electron deficient substrate, and it took longer reaction time compared to the electron rich system. The mild electron withdrawing group containing toluenes gave very good yield of the corresponding acid. Interestingly, ester and acyl substituted toluenes gave the corresponding acid products under the optimized reaction condition in very good yield without affecting the ester and the acyl group (Table 6, entries 1–3).

Highly electron deficient system such as 4-nitro toluene took longer reaction time of 48 h and yield of product 4q was also less. The methyl substituted heteroaromatic compounds gave low yield of acid product (entries 5–8).

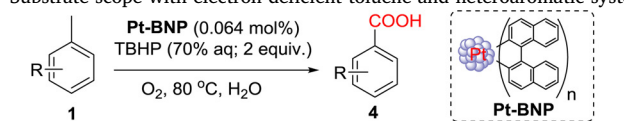
From the substrate scope, it has been observed that the electron rich toluenes afford excellent yields over electron deficient toluenes. Further, a competitive reaction was carried out using 1:1 ratio of para-methoxy toluene and para-nitro toluene. The results obtained shows that an electron rich toluene reacted faster and gave excellent yield of product, whereas electron deficient toluene performed poorly and afforded the less yield of product (Table 7, entry 1). When the TBHP equivalent was changed from 4 to 2 equivalents, electron rich toluene consumed faster and gave the corresponding acid product in good yield, whereas electron deficient toluene was consumed very slowly and gave only 2% yield of corresponding acid (entry 2).

To ensure the practical utility of the optimized reaction condition, a gram scale reaction was performed using 4-methoxy toluene (1a) which afforded promising 91% yield of the corresponding 4-methoxy benzoic acid (4a) (Scheme 2).

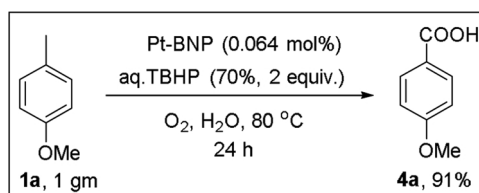
Next, an attempt was made to synthesize industrially important chemical terephthalic acid from xylene by increasing the equivalents of oxidant. When 4 equivalents of TBHP was used at a time, it gave only 7% yield (Table 8, entry 1) of p-terephthalic acid, but two portion wise addition of TBHP at 26 h intervals gave 22% yield of p-terephthalic acid as the solubility of intermediate product p-tolanic acid in water is low (entry 2). Then mixed solvent (water and AcOH (1:1)) was used to solubilise the intermediate product p-tolanic acid and the reaction gave

Table 6

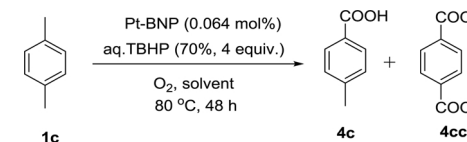
Substrate scope with electron deficient toluene and heteroaromatic system.



Entry	Toluenes	Product	Time (h)	Yield (%)
1			28	93
2			28	96
3			30	86
4			48	68
5 ^a			48	47
6 ^a			48	60
7 ^a			48	65
8 ^a			48	58

^a Yield was calculated by GC using naphthalene as internal standard.**Scheme 2.** A gram scale reaction of Pt-BNP catalyzed oxidation.**Table 8**

oxidation of xylene to terephthalic acid.



Entry	Solvent	Conversion (%)	Yield (%)	
			4c	4cc
1	H ₂ O	> 99	86	7
2 ^a	H ₂ O	> 99	70	22
3 ^a	H ₂ O:AcOH(1:1)	> 99	39	52

^a TBHP was added at 26 h intervals in two portion.

52% yield of p-terephthalic acid (Table 8, entry 3).

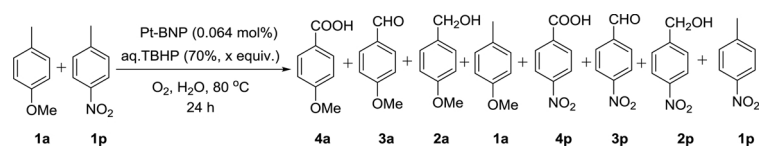
During the study of the substrate scope, it has been shown that the acyl group is well tolerated under the optimized reaction condition. Next, attempts were made to synthesize keto compound from corresponding alkyl benzene and the results are summarized in Table 9. It was found that both acyclic and cyclic system afforded the corresponding ketone in very good yields. Ethylbenzene gave 94% of corresponding acetophenone (**6a**), (entry 1). Propylbenzene afforded the corresponding propiophenone (**6b**) in 96% yield (entry 2) and cyclic system indane yielded corresponding indanone (**6c**) in 89% (entry 3). As expected the 4-ethylphenol undergoes radical polymerization under the optimized reaction condition and unable to give corresponding 4-acylphenol (**6d**) (entry 4). However, the phenylacetic acid was unable to afford the α -keto acid (**6e**) (entry 5).

Interestingly, methyl ester of phenylacetic acid **5e** gave the corresponding α -keto ester (**6f**) (entry 6) in very good yield. Further, various phenylacetic acid ester has been used for the synthesis of corresponding α -keto ester molecules. Halogen substituted such as *ortho* bromo (**5g**) and *para* bromo (**5h**) methyl ester of phenylacetic acid yielded the corresponding α -keto ester (**6g** and **6h**) in 81 and 84% respectively. Isopropyl ester of phenylacetic acid gave good yield of corresponding α -keto ester **6i** under the optimized reaction condition.

For the practical utilization of present methodology, a gram scale reaction was carried out using ethylbenzene as a substrate without

Table 7

competitive experiment with respect to electron rich and deficient toluene.

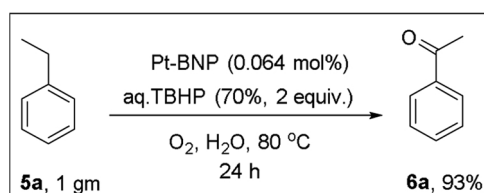
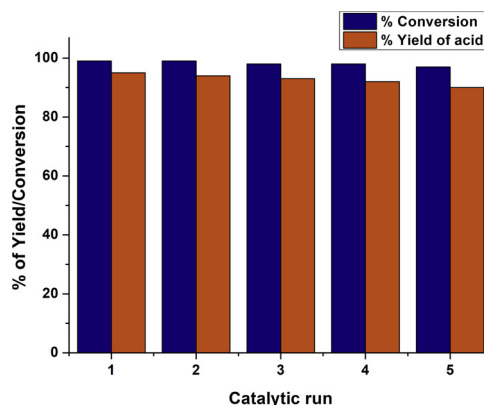


Entry	TBHP (x equiv.)	Yield (%)							
		4a	3a	2a	1a	4p	3p	2p	1p
1	4	94	1	1	0	34	2	0	60
2	2	87	2	1	3	2	1	0	94

Table 9

Pt-BNP catalyzed oxidation of alkyl benzene to aromatic ketone.

Entry	Reactant	Product	Time (h)	Yield (%)	
				% Conversion	% Yield of acid
1	5a	6a	20	94	
2	5b	6b	20	98	
3	5c	6c	24	89	
4	5d	6d	24	00	
5	5e	6e	48	00	
6	5f	6f	18	87	
7	5g	6g	20	81	
8	5h	6h	20	84	
9	5i	6i	20	80	

**Scheme 3.** A gram scale reaction of Pt-BNP catalyzed oxidation of ethyl benzene.**Fig. 10.** Recyclability test of Pt-BNP catalyst.

compromising the optimized reaction condition and gave 93% yield of corresponding acetophenone (**Scheme 3**).

For our curiosity, a competitive experiment was carried out by using 1:1 ratio of electron rich para-methoxy toluene and ethylbenzene, and the results showed (**Table 10**, entry 1) that both the starting material have similar reactivity as the reaction gave 46% of acetophenone and 41% of 4-methoxy benzoic acid. However, a competitive experiment between electrically neutral substrate such as toluene and ethylbenzene suggested that benzylic CH₂ is oxidized faster than the benzylic CH₃ (entry 2).

3.3. Stability of catalyst in the reaction medium

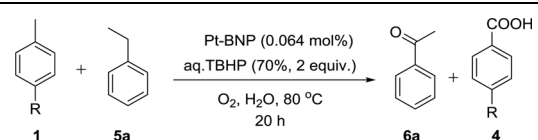
From the economical viewpoint, further efforts were made to recover and reuse the Pt-BNP catalyst. The toluene oxidation reaction was carried out at 1 mmol scale under the optimized conditions. The catalyst was recovered and reused up to five catalytic cycles and desired product 4a was isolated in the 95%, 93%, 94%, 92% and 90% yields in successive runs. The recovery (%) of Pt-BNP in each run was calculated with respect to previous run. In every run, there are some weight loss of catalyst was observed, it may be the loss of catalyst during the decantation. This result reveals that the catalytic activity remains the same as initial stage catalysts (**Fig. 10**).

Moreover, HRTEM analysis of recovered Pt-BNP catalyst after five runs showed that there was no major change in the size distribution and dispersion of the nanoparticles compared with the freshly prepared catalyst. The average size of Pt-BNP was found to be 5–8 nm (**Fig. 11**).

To prove that the active species of Pt-BNP catalyst is heterogeneous Pt, not the leached homogeneous Pt species, the heterogeneous test such as hot centrifugation test and the mercury poisoning test were carried out. In hot centrifugation test, the reaction mixture was filtered in the middle of the reaction at different time intervals, 6 h, 12 h and 18 h respectively. Then the filtrate was allowed to stir for next 30 h. It was observed that the reaction did not proceed with the filtrate. The

Table 10

competitive experiment with respect to electron rich/neutral toluene and ethylbenzene.



Entry	Toluene	Alkyl benzene	Conversion (%)		Yield (%)	
			1	5a	4	6a
1	1a	5a	48	50	41	46
2	1g	5a	24	77	19	65

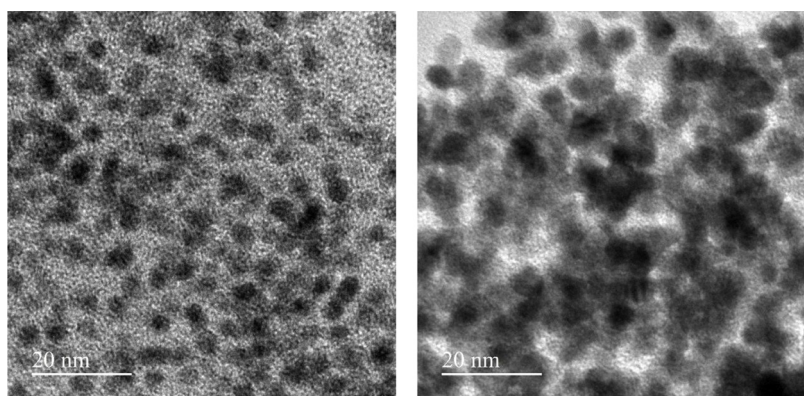


Fig. 11. HRTEM image of Pt-BNP catalyst: Fresh catalyst (left) and recycled catalyst after five runs (right).

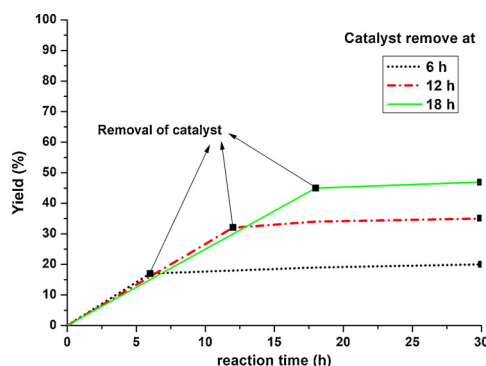
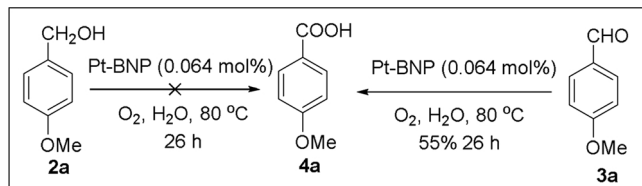
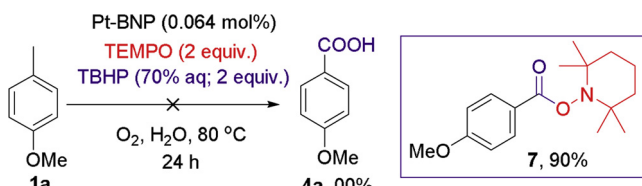


Fig. 12. Graphical representation of hot centrifugation test.



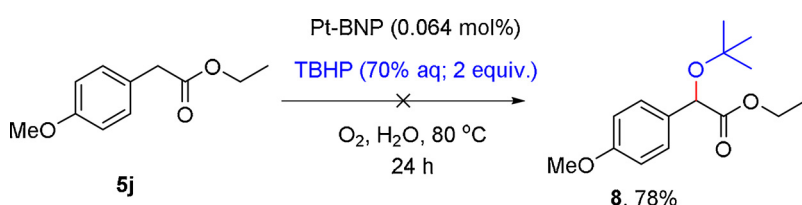
Scheme 4. Control experiments in absence of TBHP.



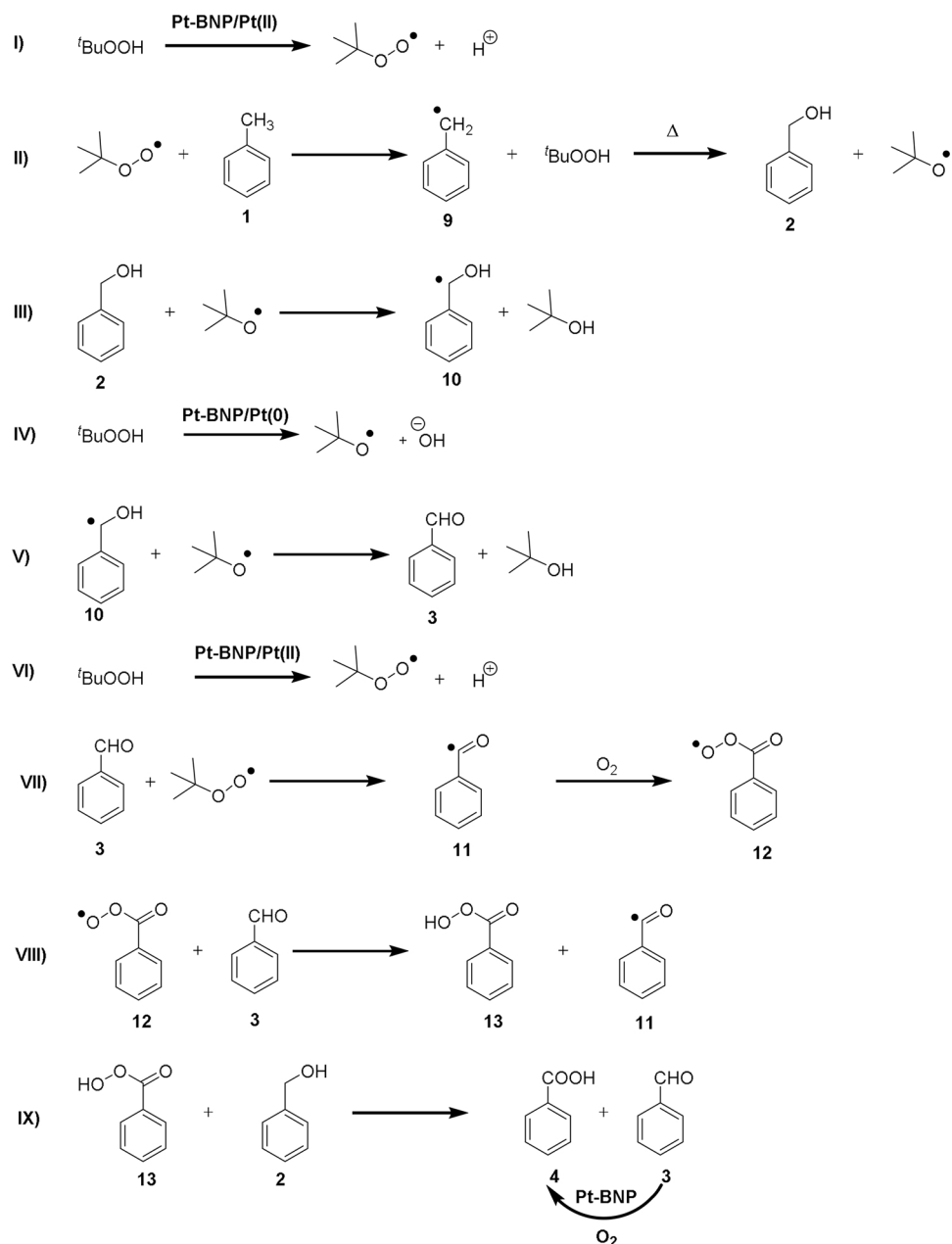
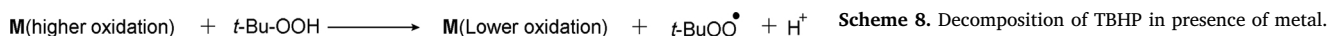
Scheme 5. Free radical trapping experiment in presence of TEMPO.

catalytic activity of residue Pt-BNP after hot filtration was similar to fresh Pt-BNP (Fig. 12).

Then, the mercury poisoning test was conducted, and results show that the Pt-BNP is heterogeneous nature in reaction medium.



Scheme 6. Tertiary butoxide intermediate trapping experiment.



Scheme 9. Possible reaction mechanism.

butoxide radical whereas in the lower oxidation state of metal generates tertiary butyl peroxy radical [83].

The oxidation of aldehyde to benzoic acid may proceed via a different pathway with complex reaction mechanism. However, based on literature reports and above control experiments, a possible reaction mechanism is proposed (Scheme 9). First, in presence of TBHP, benzyl radical **9** is generated which reacts with hydroxyl radical and give the benzyl alcohol **2** (equation II). The hydroxyl group of benzyl alcohol comes from TBHP. At the time of formation of benzyl alcohol, TBHP decomposes to corresponding tertiary butoxide radical. Then tertiary butoxide radical abstract hydrogen radical from benzyl alcohol and immediately generate tertiary butanol and benzyl alcohol radical **10**

(equation III) which is further oxidized to corresponding aldehyde **3** (equation V). The formation of benzyl alcohol and benzaldehyde during the reaction was confirmed by GC-MS analysis of reaction mixture (See Fig. 2). Then benzoyl radical **11** is generated, in presence of TBHP from benzaldehyde **3**. However, the possibility to generate benzoyl radical in presence of metal and molecular oxygen cannot be ruled out. Further, in presence of molecular oxygen, benzoyl radical gets converted to corresponding benzoylperoxy radical **12** intermediate (equation VII). The benzoylperoxy radical takes hydrogen from benzaldehyde and generates peroxy benzoic acid **13** and benzoyl radical **11** (equation VIII). Subsequently, peroxy benzoic acid generates the benzoic acid **4** (equation IX). There is another possibility to produce benzoic acid from

benzoyl radical, the benzoyl radical in presence of Pt-BNP react with hydroxyl ion and produce the corresponding acid molecule (Scheme 9). The possibility of oxidation of aldehyde to acid by TBHP cannot be ruled out. However, the actual oxidation state of Pt-BNP involved in oxidation reaction is not confirmed as Pt-BNP contain Pt(0), Pt(II) and Pt(IV).

4. Conclusion

An efficient method for Pt-BNP catalyzed sequential selective oxidation of methyl and alkylarenes to corresponding carboxylic acid and ketone with high conversion under mild reaction condition has been developed. This methodology has been successfully utilized for the oxidation of less reactive electron deficient toluenes to the corresponding acid. In this methodology, easily accessible petroleum by-product toluene, and greener oxidant TBHP were used for the oxidation. The toluene oxidation reaction has proceeded in presence of 0.064 mol % of Pt-BNP catalyst in water. The synthesized Pt-BNP catalyst has shown high TON (738-1448) for selective oxidation of toluene to benzoic acid. The Pt-BNP catalyst was reused up to six catalytic cycles without any major change in particle size and activity. Mercury poisoning test and hot centrifugation test confirmed that the reaction is catalyzed by heterogeneous Pt-BNP and not by leached homogeneous Pt.

Acknowledgements

G.S thanks IIT Madras for exploratory research project (CHY/16-17/846/RFER/GSEK) and SERB-DST for funding. R.S thanks IIT Madras for senior research fellowship.

Appendix A. Supplementary data

Supplementary material related to this article can be found, in the online version, at doi:<https://doi.org/10.1016/j.apcatb.2019.03.052>.

References

- V. Parvulescu, C. Anastasescu, C. Constantin, B.L. Su, Highly selective oxidation of aromatic hydrocarbons (styrene, benzene and toluene) with H_2O_2 over Ni, Ni-Cr and Ni-Ru modified MCM-41 catalysts, in: R. Aiello, G. Giordano, F. Testa (Eds.), *Studies in Surface Science and Catalysis*, Vol. 142 Elsevier, 2002, pp. 1213–1220.
- C.R. Downs, Oxidation of aromatic hydrocarbons, *Ind. Eng. Chem.* 32 (1940) 1294–1298.
- B. Yang, Z. Fu, A. Su, J. She, M. Chen, S. Tang, W. Hu, C. Zhang, Y. Liu, Influence of tetraalkylammonium cations on quality of decatungstate and its photocatalytic property in visible light-triggered selective oxidation of organic compounds by di-oxygens, *Appl. Catal. B* 242 (2019) 249–257.
- M. Qamar, R.B. Elsayed, K.R. Alhooshani, M.I. Ahmed, D.W. Bahnemann, Highly Efficient and selective oxidation of aromatic alcohols photocatalyzed by nanoporous hierarchical Pt/Bi2W06 in organic solvent-free environment, *ACS Appl. Mater. Interfaces* 7 (2015) 1257–1269.
- L. Chen, J. Tang, L.-N. Song, P. Chen, J. He, C.-T. Au, S.-F. Yin, Heterogeneous photocatalysis for selective oxidation of alcohols and hydrocarbons, *Appl. Catal. B* 242 (2019) 379–388.
- L. Torrente-Murciano, A. Gilbank, B. Puerolas, T. Garcia, B. Solsona, D. Chadwick, Shape-dependency activity of nanostructured CeO₂ in the total oxidation of polycyclic aromatic hydrocarbons, *Appl. Catal. B* 132–133 (2013) 116–122.
- D.D. Mal, S. Khilari, D. Pradhan, Efficient and selective oxidation of toluene to benzaldehyde on manganese tungstate nanobars: a noble metal-free approach, *Green Chem.* 20 (2018) 2279–2289.
- H.-G. Franck, J.W. Stadelhofer, Production and uses of toluene derivatives, in: H.-G. Franck, J.W. Stadelhofer (Eds.), *Industrial Aromatic Chemistry: Raw Materials Processes Products*, Springer, Berlin, Heidelberg, 1988, pp. 236–264.
- G.R. Bertolini, L.R. Pizzio, A. Kubacka, M.J. Muñoz-Batista, M. Fernández-García, Composite H3PW12O40–TiO₂ catalysts for toluene selective photo-oxidation, *Appl. Catal. B* 225 (2018) 100–109.
- J. Wu, Q. Xia, H. Wang, Z. Li, Catalytic performance of plasma catalysis system with nickel oxide catalysts on different supports for toluene removal: effect of water vapor, *Appl. Catal. B* 156–157 (2014) 265–272.
- Z. Ye, J.M. Giraudon, N. Nuns, P. Simon, N. De Geyter, R. Morent, J.F. Lamontier, Influence of the preparation method on the activity of copper-manganese oxides for toluene total oxidation, *Appl. Catal. B* 223 (2018) 154–166.
- M.J. Muñoz-Batista, G.R. Bertolini, C.I. Cabello, R. Luque, E. Rodríguez-Castellón, A. Kubacka, M. Fernández-García, Novel (NH4)4[NiMo6O24H6]·5H2O–TiO₂ composite system: photo-oxidation of toluene under UV and sunlight-type illumination, *Appl. Catal. B* 238 (2018) 381–392.
- X. Wang, J. Wu, M. Zhao, Y. Lv, G. Li, C. Hu, Partial oxidation of toluene in CH_3COOH by H_2O_2 in the presence of $VO(acac)_2$ catalyst, *J. Phys. Chem. C* 113 (2009) 14270–14278.
- W.W. Kaeding, R.O. Lindblom, R.G. Temple, H.I. Mahon, Oxidation of toluene and other alkylated aromatic hydrocarbons to benzoic acids and phenols, *Ind. Eng. Chem. Process Des. Dev.* 4 (1965) 97–101.
- J. Mo, Y. Zhang, Q. Xu, Y. Zhu, J.J. Lamson, R. Zhao, Determination and risk assessment of by-products resulting from photocatalytic oxidation of toluene, *Appl. Catal. B* 89 (2009) 570–576.
- P.M. Davidson, J.N. Sofos, A.L. Branen, *Antimicrobials in Food*, 3rd ed., CRC Press, Taylor & Francis, U.S., 2005.
- J.E. Fearn, J.B. DeWitt, Correlation between chemical structure and rodent repellency of benzoic acid derivatives, *J. Agric. Food Chem.* 13 (1965) 116–117.
- A.T. Allan, M. Finch, C. Maddison, K.L. Robone, M. Sharples, Insect-Repellent Compositions Comprising Antimicrobial Agents and Non Ionic Surfactants, WO1997043369A1 (1997).
- E.M. Adams, Insect Repellent, US2000004A (1935).
- J. Kuljiraseth, A. Wangriya, J.M.C. Malones, W. Klysubun, S. Jitkarnka, Synthesis and characterization of AMO LDH-derived mixed oxides with various Mg/Al ratios as acid–basic catalysts for esterification of benzoic acid with 2-ethylhexanol, *Appl. Catal. B* 243 (2019) 415–427.
- G. Brătescu, Y. Le Bigot, M. Delmas, New method for synthesis of benzoic acid, *Rev. Chim. (Bucharest)* 51 (2000) 357–358.
- Y. Yan, Y. Chen, X. Jia, Y. Yang, Palladium nanoparticles supported on organosilane-functionalized carbon nanotube for solvent-free aerobic oxidation of benzyl alcohol, *Appl. Catal. B* 156–157 (2014) 385–397.
- S. Bota, A. Caraban, G. Gavris, A. Cozma, Study for optimized oxidation process of the synthesis of benzoic acid, *An. Univ. Oradea, Fasc. Chim.* 16 (2009) 86–90.
- X. Dai, M. Xie, S. Meng, X. Fu, S. Chen, Coupled systems for selective oxidation of aromatic alcohols to aldehydes and reduction of nitrobenzene into aniline using CdS/g-C3N4 photocatalyst under visible light irradiation, *Appl. Catal. B* 158–159 (2014) 382–390.
- K. Tamai, S. Hosokawa, K. Teramura, T. Shishido, T. Tanaka, Synthesis of niobium oxide nanoparticles with plate morphology utilizing solvothermal reaction and their performances for selective photooxidation, *Appl. Catal. B* 182 (2016) 469–475.
- F. Arena, B. Guminia, C. Cannilla, L. Spadaro, A. Patti, L. Spiccia, Nanostructured MnO_x catalysts in the liquid phase selective oxidation of benzyl alcohol with oxygen: Part II. Reaction mechanism, kinetics and deactivation pattern, *Appl. Catal. B* 170–171 (2015) 233–240.
- Y. Zhu, H. Wang, B. Wang, X. Liu, H. Wu, S. Licht, Solar thermoelectric field plus photocatalysis for efficient organic synthesis exemplified by toluene to benzoic acid, *Appl. Catal. B* 193 (2016) 151–159.
- T. Lu, Y. Mao, K. Yao, J. Xu, M. Lu, Metal free: A novel and efficient aerobic oxidation of toluene derivatives catalyzed by N',N'',N'''-trihydroxyisocyanuric acid and dimethylglyoxime in PEG-1000-based dicationic acidic ionic liquid, *Catal. Commun.* 27 (2012) 124–128.
- N. Hirai, N. Sawatari, N. Nakamura, S. Sakaguchi, Y. Ishii, Oxidation of substituted toluenes with molecular oxygen in the presence of N,N',N'''-trihydroxyisocyanuric acid as a key catalyst, *J. Org. Chem.* 68 (2003) 6587–6590.
- J. Fraga-Dubreuil, E. Garcia-Verdugo, P.A. Hamley, E.M. Vaquero, L.M. Dudd, I. Pearson, D. Housley, W. Partenheimer, W.B. Thomas, K. Whiston, M. Poliakoff, Catalytic selective partial oxidations using O_2 in supercritical water: the continuous synthesis of carboxylic acids, *Green Chem.* 9 (2007) 1238–1245.
- B.K. Sharma, *Industrial Chemistry Including Chemical Engineering*, Goel Publishing House, Meerut, 1997 ISBN 8187224002.
- T.V. Bukharkina, N.D. Gavrilenko, N.G. Diguurov, N.A. Knyazeva, Kinetics of the oxidation of toluene in acetic acid by cobalt(III) and manganese(III) salts in the presence of sodium bromide, *Kinet. Katal.* 19 (1978) 506–510.
- A.M. Ivanov, Oxidation of toluene in acetic acid, *Zh. Prikl. Khim. (Leningrad)* 47 (1974) 1830–1834.
- N.G. Diguurov, E.V. Shevryeva, Oxidation of toluene with a cobalt-manganese-bromide catalyst in an acetic acid solution, *Mosk. Khim.-Tekhnol. Inst.* (1980) 14 pp.
- D.A. Bulushev, F. Rainone, L. Kiwi-Minsker, Partial oxidation of toluene to benzaldehyde and benzoic acid over model vanadia/titania catalysts: role of vanadia species, *Catal. Today* 96 (2004) 195–203.
- C.L. Bianchi, S. Gatto, C. Pirola, A. Naldoni, A. Di Michele, G. Cerrato, V. Crocellà, V. Capucci, Photocatalytic degradation of acetone, acetaldehyde and toluene in gas-phase: Comparison between nano and micro-sized TiO₂, *Appl. Catal. B* 146 (2014) 123–130.
- N. Keller, E. Barraud, F. Bosc, D. Edwards, V. Keller, On the modification of photocatalysts for improving visible light and UV degradation of gas-phase toluene over TiO₂, *Appl. Catal. B* 70 (2007) 423–430.
- A.J. Maira, K.L. Yeung, J. Soria, J.M. Coronado, C. Belver, C.Y. Lee, V. Augugliaro, Gas-phase photo-oxidation of toluene using nanometer-size TiO₂ catalysts, *Appl. Catal. B* 29 (2001) 327–336.
- S. Li, B. Liang, S. Tang, Liquid phase oxidation of toluene catalyzed by Co/Mn/Zr composite catalyst, *Huaxue Fanying Gongcheng Yu Gongyi* 28 (2012) 143–148 163.
- J. Gao, Z. Si, Y. Xu, L. Liu, Y. Zhang, X. Wu, R. Ran, D. Weng, Pd-Ag@CeO₂ catalyst of core-shell structure for low temperature oxidation of toluene under visible light irradiation, *J. Phys. Chem. C* 123 (2019) 1761–1769.
- S.K. Jesudoss, J.J. Vijaya, M. Sivachidambaram, L.J. Kennedy, R. Jothiramalingam, H.A. Al-Lohedan, Liquid phase catalytic oxidation of toluene over rich silica and

alumina composition of hierarchical ordered ZSM-5 zeolites prepared without organic templates, *J. Nanosci. Nanotechnol.* 18 (2018) 5367–5379.

[42] F. Wang, J. Xu, X. Li, J. Gao, L. Zhou, R. Ohnishi, Liquid phase oxidation of toluene to benzaldehyde with molecular oxygen over copper-based heterogeneous catalysts, *Adv. Synth. Catal.* 347 (2005) 1987–1992.

[43] F. Konietzni, U. Kolb, U. Dingerdissen, W.F. Maier, AMM-MnxSi-catalyzed selective oxidation of toluene, *J. Catal.* 176 (1998) 527–535.

[44] D.E. Collinn, F.A. Richery, J.A. Kent (Ed.), *Reigle Handbook of Industrial Chemistry*, ed. 1987, C.B.S, New Delhi, 2019Ch. 22.

[45] K. Weissermel, H.J. Arpe, *Industrial Organic Chemistry*, fourth edition, Wiley-VCH, Weinheim, 2003.

[46] L. Zhao, Z. Zhang, Y. Li, X. Leng, T. Zhang, F. Yuan, X. Niu, Y. Zhu, Synthesis of CeAlMnO_x hollow microsphere with hierarchical structure and its excellent catalytic performance for toluene combustion, *Appl. Catal. B* 245 (2019) 502–512.

[47] G. Busca, Chapter 1 – heterogeneous catalysts, in: G. Busca (Ed.), *Heterogeneous Catalytic Materials*, Elsevier, Amsterdam, 2014, pp. 1–7.

[48] S.O. Ganiyu, M. Zhou, C.A. Martínez-Huitle, Heterogeneous electro-Fenton and photoelectro-Fenton processes: a critical review of fundamental principles and application for water/wastewater treatment, *Appl. Catal. B* 235 (2018) 103–129.

[49] P. Hu, M. Long, Cobalt-catalyzed sulfate radical-based advanced oxidation: a review on heterogeneous catalysts and applications, *Appl. Catal. B* 181 (2016) 103–117.

[50] M.E. Borges, L. Díaz, M.C. Alvarez-Galván, A. Brito, High performance heterogeneous catalyst for biodiesel production from vegetal and waste oil at low temperature, *Appl. Catal. B* 102 (2011) 310–315.

[51] R. Raja, J.M. Thomas, V. Dreyer, Benign oxidants and single-site solid catalysts for the solvent-free selective oxidation of toluene, *Catal. Lett.* 110 (2006) 179–183.

[52] Y. Li, J. Huang, X. Hu, F.L.-Y. Lam, W. Wang, R. Luque, Heterogeneous Pd catalyst for mild solvent-free oxidation of benzyl alcohol, *J. Mol. Catal. A Chem.* 425 (2016) 61–67.

[53] Z. Sihai, F. Puleo, J.M. Garcia-Vargas, L. Retailleau, C. Descorme, L.F. Liotta, J.L. Valverde, S. Gil, A. Giroir-Fendler, Manganese oxide-based catalysts for toluene oxidation, *Appl. Catal. B* 209 (2017) 689–700.

[54] A. Giroir-Fendler, M. Alves-Fortunato, M. Richard, C. Wang, J.A. Díaz, S. Gil, C. Zhang, F. Can, N. Bion, Y. Guo, Synthesis of oxide supported LaMnO₃ perovskites to enhance yields in toluene combustion, *Appl. Catal. B* 180 (2016) 29–37.

[55] T. Barakat, V. Idakiev, R. Cousin, G.S. Shao, Z.Y. Yuan, T. Tabakova, S. Sifert, Total oxidation of toluene over noble metal based Ce, Fe and Ni doped titanium oxides, *Appl. Catal. B* 146 (2014) 138–146.

[56] O. Pliekhov, O. Pliekhova, U. Lavrencic Stangar, N. Zabukovec Logar, The Co-MOF-74 modified with N,N'-dihydroxypyromellitimide for selective, solvent free aerobic oxidation of toluene, *Catal. Commun.* 110 (2018) 88–92.

[57] T.W. Bastock, J.H. Clark, K. Martin, B.W. Trenbirth, Mild, solvent-free oxidation of toluene and substituted toluenes to their benzoic acids using carboxylic acid-promoted heterogeneous catalysis, *Green Chem.* 4 (2002) 615–617.

[58] F. Wang, J. Xu, X. Li, J. Gao, L. Zhou, R. Ohnishi, Liquid phase oxidation of toluene to benzaldehyde with molecular oxygen over copper-based heterogeneous catalysts, *Adv. Synth. Catal.* 347 (2005) 1987–1992.

[59] Y. Li, J. Huang, X. Hu, F.L.-Y. Lam, W. Wang, R. Luque, Heterogeneous Pd catalyst for mild solvent-free oxidation of benzyl alcohol, *J. Mol. Catal. A Chem.* 425 (2016) 61–67.

[60] G. Savitha, R. Saha, G. Sekar, Bimetallic chiral nanoparticles as catalysts for asymmetric synthesis, *Tetrahedron Lett.* 57 (2016) 5168–5178.

[61] A. Akbari, M. Amini, A. Tarassoli, B. Eftekhari-Sis, N. Ghasemian, E. Jabbari, Transition metal oxide nanoparticles as efficient catalysts in oxidation reactions, *Nano-Struct. Nano-Objects* 14 (2018) 19–48.

[62] K. Kaneda, T. Mizugaki, Design of high-performance heterogeneous catalysts using apatite compounds for liquid-phase organic syntheses, *ACS Catal.* 7 (2017) 920–935.

[63] H. Zhou, H. Xu, Y. Liu, Aerobic oxidation of 5-hydroxymethylfurfural to 2,5-furandicarboxylic acid over Co/Mn-lignin coordination complexes-derived catalysts, *Appl. Catal. B* 244 (2019) 965–973.

[64] T. Rafaideen, S. Baranton, C. Coutanceau, Highly efficient and selective electro-oxidation of glucose and xylose in alkaline medium at carbon supported alloyed PdAu nanocatalysts, *Appl. Catal. B* 243 (2019) 641–656.

[65] M.N. Krstajić Pajić, S.I. Stevanović, V.V. Radmilović, A. Gavrilović-Wohlmuther, P. Zabinski, N.R. Elezović, V.R. Radmilović, S.L. Gojković, V.M. Jovanović, Dispersion effect in formic acid oxidation on PtAu/C nanocatalyst prepared by water-in-oil microemulsion method, *Appl. Catal. B* 243 (2019) 585–593.

[66] L. Kesavan, R. Tiruvalam, M.H. Ab Rahim, M.I. bin Saiman, D.I. Enache, R.L. Jenkins, N. Dimitratos, J.A. Lopez-Sánchez, S.H. Taylor, D.W. Knight, C.J. Kiely, G.J. Hutchings, Solvent-free oxidation of primary carbon-hydrogen bonds in toluene using Au-Pd alloy nanoparticles, *Science* 331 (2011) 195–199.

[67] K.T.V. Rao, P.S.N. Rao, P. Nagaraju, P.S.S. Prasad, N. Lingaiah, Room temperature selective oxidation of toluene over vanadium substituted polyoxometalate catalysts, *J. Mol. Catal. A Chem.* 303 (2009) 84–89.

[68] M.I. bin Saiman, G.L. Brett, R. Tiruvalam, M.M. Forde, K. Sharples, A. Thetford, R.L. Jenkins, N. Dimitratos, J.A. Lopez-Sánchez, D.M. Murphy, D. Bethell, D.J. Willock, S.H. Taylor, D.W. Knight, C.J. Kiely, G.J. Hutchings, Involvement of surface-bound radicals in the oxidation of toluene using supported Au-Pd nanoparticles, *Angew. Chem. Int. Ed.* 51 (2012) 5981–5985 S5981/S5981/5910.

[69] R. Burch, P.K. Loader, F.J. Urbano, Some aspects of hydrocarbon activation on platinum group metal combustion catalysts, *Catal. Today* 27 (1996) 243–248.

[70] C. Donze, P. Korovchenko, P. Gallezot, M. Besson, Aerobic selective oxidation of (hetero)aromatic primary alcohols to aldehydes or carboxylic acids over carbon supported platinum, *Appl. Catal. B* 70 (2007) 621–629.

[71] L.Q. Wang, M. Bevilacqua, J. Filippi, P. Fornasiero, M. Innocenti, A. Lavacchi, A. Marchionni, H.A. Miller, F. Vizza, Electrochemical growth of platinum nanostructures for enhanced ethanol oxidation, *Appl. Catal. B* 165 (2015) 185–191.

[72] R. Chang, L. Zheng, C. Wang, D. Yang, G. Zhang, S. Sun, Synthesis of hierarchical platinum-palladium-copper nanodendrites for efficient methanol oxidation, *Appl. Catal. B* 211 (2017) 205–211.

[73] E. Antolini, Photo-assisted methanol oxidation on Pt-TiO₂ catalysts for direct methanol fuel cells: a short review, *Appl. Catal. B* 237 (2018) 491–503.

[74] K. Leistner, C. Gonzalez Braga, A. Kumar, K. Kamasamudram, L. Olsson, Volatilisation and subsequent deposition of platinum oxides from diesel oxidation catalysts, *Appl. Catal. B* 241 (2014) 338–350.

[75] J.M. Herreros, S.S. Gill, I. Lefort, A. Tsolakis, P. Millington, E. Moss, Enhancing the low temperature oxidation performance over a Pt and a Pt-Pd diesel oxidation catalyst, *Appl. Catal. B* 147 (2014) 835–841.

[76] S.K. Moromi, S.M.A. Hakim Siddiki, M.A. Ali, K. Kon, K.-i. Shimizu, Acceptorless dehydrogenative coupling of primary alcohols to esters by heterogeneous Pt catalysts, *Catal. Sci. Technol.* 4 (2014) 3631–3635.

[77] D. Ganapathy, G. Sekar, Palladium nanoparticles stabilized by metal–carbon covalent bond: An efficient and reusable nanocatalyst in cross-coupling reactions, *Catal. Commun.* 39 (2013) 50–54.

[78] N. Parveen, R. Saha, G. Sekar, Stable and reusable palladium nanoparticles-catalyzed conjugate addition of aryl iodides to enones: route to reductive Heck products, *Adv. Synth. Catal.* 359 (2017) 3741–3751.

[79] R. Saha, D. Arunprasad, G. Sekar, Phosphine-free and reusable palladium nanoparticles-catalyzed domino strategy: synthesis of indanone derivatives, *J. Org. Chem.* 83 (2018) 4692–4702.

[80] R. Saha, G. Sekar, Stable Pd-nanoparticles catalyzed domino C–H activation/C–N bond formation strategy: an access to phenanthridinones, *J. Catal.* 366 (2018) 176–188.

[81] R. Saha, N. Perveen, N. Nihesh, G. Sekar, Reusable palladium nanoparticles catalyzed oxime ether directed mono ortho-hydroxylation under phosphine free neutral condition, *Adv. Synth. Catal.* (2018), <https://doi.org/10.1002/adsc.201801340>.

[82] B.M. Still, P.G.A. Kumar, J.R. Aldrich-Wright, W.S. Price, ¹⁹⁵Pt NMR-theory and application, *Chem. Soc. Rev.* 36 (2007) 665–686.

[83] G. Rothenberg, L. Feldberg, H. Wiener, Y. Sasson, Copper-catalyzed homolytic and heterolytic benzylic and allylic oxidation using tert-butyl hydroperoxide, *J. Chem. Soc. Perkin Trans. I* 2 (1998) 2429–2434.